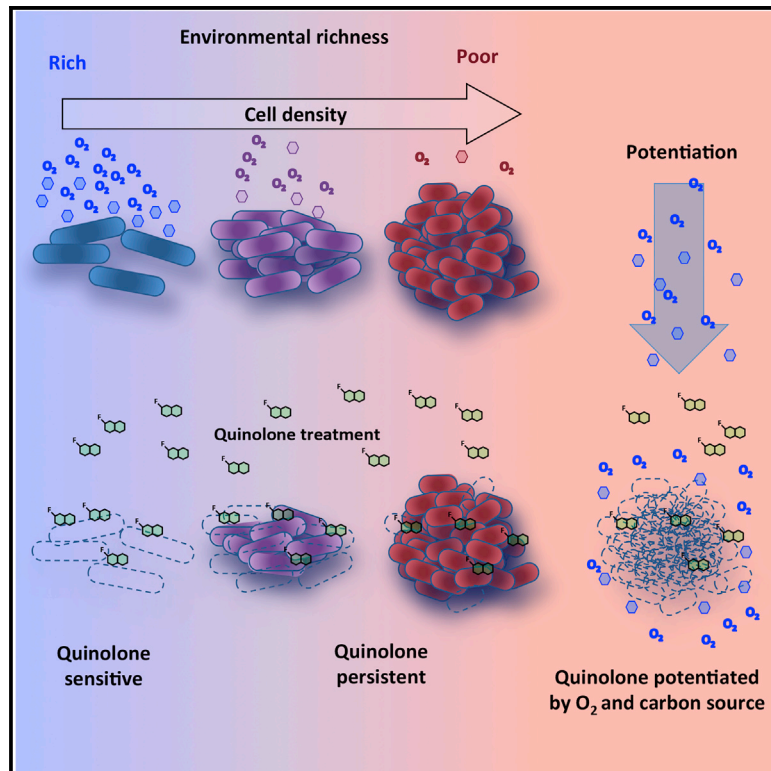


Molecular Cell

Understanding and Sensitizing Density-Dependent Persistence to Quinolone Antibiotics

Graphical Abstract



Authors

Arnaud Gutierrez, Saloni Jain,
Perna Bhargava, Meagan Hamblin,
Michael A. Lobritz, James J. Collins

Correspondence

jimjc@mit.edu

In Brief

Gutierrez et al. show that activation of cellular respiration is sufficient to sensitize antibiotic refractory bacteria at high densities to drugs targeting DNA topoisomerases. This suggests that the nutrient environment and metabolic state are key components of bacterial persistence phenotypes.

Highlights

- Quinolone antibiotics fail to kill bacterial populations at high density
- Exhaustion of OXPHOS substrates drives bacterial persistence
- Carbon and electron acceptor supplementation restores antibiotic activity
- Metabolic priming of OXPHOS reverses tolerance in diverse bacterial species



Understanding and Sensitizing Density-Dependent Persistence to Quinolone Antibiotics

Arnaud Gutierrez,^{1,2,7} Saloni Jain,^{1,2,6,7} Prerna Bhargava,^{1,2} Meagan Hamblin,² Michael A. Lobritz,^{1,2,3,4} and James J. Collins^{1,2,3,5,8,*}

¹Institute for Medical Engineering & Science, Department of Biological Engineering, and Synthetic Biology Center, Massachusetts Institute of Technology, Cambridge, MA 02139, USA

²Broad Institute of MIT and Harvard, Cambridge, MA 02139, USA

³Wyss Institute for Biologically Inspired Engineering, Harvard University, Boston, MA 02115, USA

⁴Division of Infectious Diseases, Massachusetts General Hospital, Boston, MA 02114, USA

⁵Harvard-MIT Program in Health Sciences and Technology, Cambridge, MA 02139, USA

⁶Department of Biomedical Engineering, Boston University, Boston, MA 02115, USA

⁷These authors contributed equally

⁸Lead Contact

*Correspondence: jimjc@mit.edu

<https://doi.org/10.1016/j.molcel.2017.11.012>

SUMMARY

Physiologic and environmental factors can modulate antibiotic activity and thus pose a significant challenge to antibiotic treatment. The quinolone class of antibiotics, which targets bacterial topoisomerases, fails to kill bacteria that have grown to high density; however, the mechanistic basis for this persistence is unclear. Here, we show that exhaustion of the metabolic inputs that couple carbon catabolism to oxidative phosphorylation is a primary cause of growth phase-dependent persistence to quinolone antibiotics. Supplementation of stationary-phase cultures with glucose and a suitable terminal electron acceptor to stimulate respiratory metabolism is sufficient to sensitize cells to quinolone killing. Using this approach, we successfully sensitize high-density populations of *Escherichia coli*, *Staphylococcus aureus*, and *Mycobacterium smegmatis* to quinolone antibiotics. Our findings link growth-dependent quinolone persistence to discrete impairments in respiratory metabolism and identify a strategy to kill non-dividing bacteria.

INTRODUCTION

Antibiotics are the main tools to treat infectious diseases caused by bacteria; however, effective therapy is limited by the ability of bacterial populations to escape lethal drug challenges. The evasion of antibiotic stress by bacteria is receiving extensive attention by the scientific community (Van den Bergh et al., 2017). In particular, characterizing and classifying the

causes of antibiotic failure has been a recent focus (Brauner et al., 2016). These distinct classes include: antibiotic resistance, characterized by a change in the minimal inhibitory concentration; antibiotic tolerance, characterized by a change in killing kinetics; and antibiotic persistence, characterized by the presence of a time-dependent, bi-phasic killing profile. Bacterial resistance conferred by genetically encoded factors such as efflux pumps, drug-inactivating enzymes, or drug-target mutations is generally well understood, while the latter processes remain poorly characterized (Balaban et al., 2013; Bush et al., 2011). Antibiotic treatment failure associated with bacterial tolerance and persistence is relevant to many infection types, including prosthetic implant-related infections caused by *Staphylococcus aureus* or pulmonary infections caused by *Mycobacterium tuberculosis* (Fauvart et al., 2011). Importantly, drug tolerance and persistence have been identified as physiologic states that can promote the development of genetic resistance (Levin-Reisman et al., 2017), further underscoring the need to understand the biological basis for these phenomena.

Many early investigations into phenotypic tolerance and persistence found links to intrinsic genetic factors, including toxin-antitoxin modules and stress-response regulators (Dörr et al., 2010; Moyed and Bertrand, 1983). However, none of these factors could fully account for the variety and magnitude of observed phenotypes. More recently, stress responses related to extrinsic environmental cues, such as the starvation-induced stringent response (SOS), have been identified as drivers of antibiotic treatment failure (Dörr et al., 2009; Maisonneuve et al., 2013). This concept suggests the importance of the bacterial growth environment as a modulating factor of antibiotic efficacy (Harms et al., 2016). Consistent with this, attempts to potentiate aminoglycoside activity have focused on metabolic stimulation (Allison et al., 2011; Barraud et al., 2013; Knudsen et al., 2013; Meylan et al., 2017; Peng et al., 2015). In these studies, bacteria were sensitized



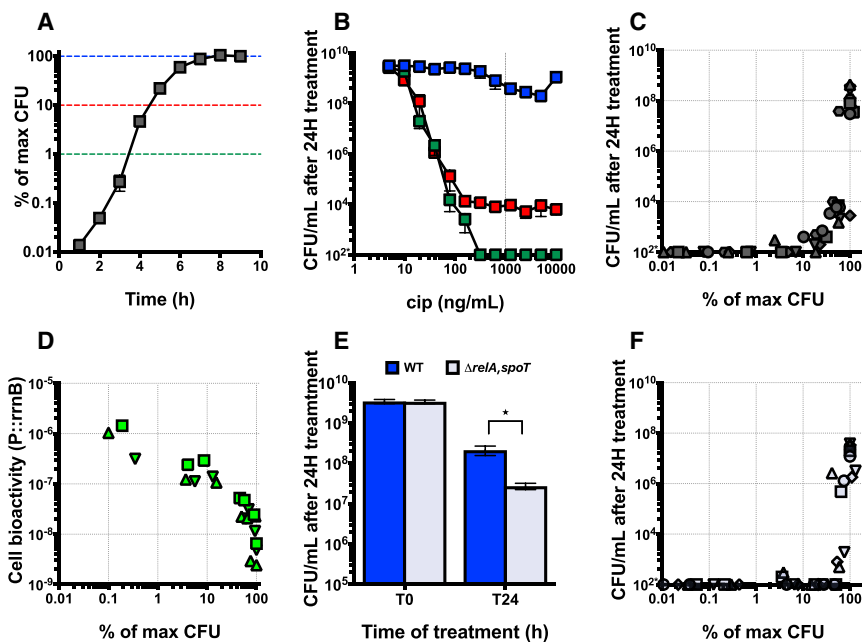


Figure 1. *E. coli* Density-Dependent Persistence to Cipro

(A) *E. coli* growth in LB medium over time (mean \pm SEM, $n = 7$). Dashed lines represent the cell density sampling (green, 1%; red, 10%; blue, 100%) of the maximum density.

(B) Cipro dose response of *E. coli* (mean \pm SEM, $n = 3$) from culture at different cell density: green, 1%; red, 10%; blue, 100% of the maximum density. The dashed line highlights the concentration of 1 $\mu\text{g}/\text{mL}$, which is used in the future sets of experiments.

(C) Density-dependent persistence to 1 $\mu\text{g}/\text{mL}$ cipro.

(D) Density-dependent expression of GFP by the P1*rrmB* promoter.

(E) Sensitivity to 1 $\mu\text{g}/\text{mL}$ cipro of the ppGpp⁰ mutant in stationary-phase culture (mean \pm SEM, $n = 3$; * Mann-Whitney, $p < 0.05$).

(F) Density-dependent persistence to 1 $\mu\text{g}/\text{mL}$ cipro of the ppGpp⁰ mutant.

In (B), (C), and (F), 10^{2*} shows our limit of detection. In (C), (D), and (F), each symbol represents a different biological replicate.

exclusively to the aminoglycoside class of antibiotics by stimulation of proton motive force-dependent antibiotic uptake. Others have shown metabolic potentiation of daptomycin, an external cell membrane-active antibiotic (Prax et al., 2016). Here, we investigate a specific manifestation of persistence characterized by cell-density-dependent drug failure. This form of persistence is hallmarked by the reduction of drug efficacy when challenging high-cell-density populations. While persister cells are often characterized using killing as a function of the drug incubation time, we define density-dependent persistence (DDP) as dose-dependent reduction in drug efficacy as a function of the initial cell density.

To assess mechanisms of DDP, we used antibiotics from the quinolone family, which are known to be affected by the density of the cell population (Zeiler, 1985). Quinolone-induced lethality derives from the poisoning of the type II topoisomerases, DNA gyrase and topoisomerase IV, which is proposed to drive DNA fragmentation leading to cell death (Drlica et al., 2008). Though binding and corruption of type II topoisomerases are essential for quinolone-induced bacterial cell death, additional factors, such as byproducts of cellular respiration and metabolism, have been implicated in bactericidal properties of quinolones (Dwyer et al., 2014, 2015). Underscoring the metabolic element of drug efficacy, the modulation of quinolone antibiotic activity against both *Escherichia coli* and *S. aureus* has been linked to the ability of cells to produce ATP (Conlon et al., 2016; Shan et al., 2017). Here, we show that metabolite exhaustion is the major driver in quinolone DDP and develop a strategy to sensitize metabolically limited, high-density cultures of bacteria to quinolones. This approach may have broad applicability to non-dividing bacterial infections and significantly impact the utility of quinolone antibiotics in the treatment of clinical bacterial infections.

RESULTS

Ciprofloxacin Activity against *E. coli* Is Dependent on Growth Phase

Ciprofloxacin (cipro) is a widely used second-generation quinolone. With a minimum inhibitory concentration (MIC) of 8–10 ng/mL in rich LB medium targeting *E. coli* strain MG1655, it is one of the most potent drugs of the quinolone family. However, the lethal effect of cipro decreases as the bacterial population grows to higher cell density (Figures 1A–1C). Alternative fluoroquinolones from the third generation (levofloxacin) and fourth generation (moxifloxacin) show similar density-dependent effects (Figures S3D and S3E). Quinolone potency is highest during exponential growth at low cell density (< 1% of maximal growth) and starts to reduce as soon as cells reach 10% of the maximal carrying capacity in LB media (around 10^8 cells). This DDP is characterized by the inability of cipro to kill a fraction of the cell population, even with a dose representing 1,000 \times the MIC and a treatment time of 24 hr (Figure 1B). The fraction of surviving cells significantly increases upon entry into stationary phase (Figures 1A–1C) and represents 10%–100% of the population depending on the drug concentration used for the treatment.

In order to study DDP to cipro in more detail, we tested a range of cultivation conditions. We treated cells with 1 $\mu\text{g}/\text{mL}$ cipro (100 \times MIC), as this concentration achieved maximal killing at low cell density and retained cell killing at intermediate cell density (Figure 1B). We further conducted our experiments in MOPS-rich media to ensure that the DDP observed in LB is conserved across discrete growth conditions (Figures S1A–S1C). Consistent with previous reports, we found that an initial dilution of 1/10,000 from overnight cultures was necessary to avoid pre-existing cells being able to persist to our concentration range (Figures S1D and S1E) (Brauner et al., 2016).

To exclude the possibility that DDP to cipro was entirely a consequence of impaired drug uptake, we examined density-dependent susceptibility of a quinolone-hypersensitive mutant, *recB*, which is unable to repair DNA double-stranded breaks. This mutant is still hypersensitive in stationary phase (Figures S1F and S1G), suggesting that DDP to cipro is not exclusively due to reduced diffusion of the drug. We confirmed these data by performing uptake measurements of cipro by stationary-phase cells (Figure S1H). We found that within 30 min, stationary-phase bacteria were able to accumulate cipro in a dose-dependent manner. From this finding, we hypothesized that stationary-phase cells may still be damaged by quinolones; however, the damage leads to limited cell death in wild-type cells under these conditions. We thus hypothesized that environmental constraints could be an additional factor in quinolone DDP.

To test this hypothesis, we examined the expression of an unstable GFP variant under the control of the ribosomal RNA promoter P1 (*P1rrnB*) (Maisonneuve et al., 2013; Mathieu et al., 2016), the activity of which has been shown to correlate with the overall ability of the cells to grow as well as the formation of persister cells. We observed a gradual decrease in GFP expression as the cell population increased, followed by a steep drop in fluorescence corresponding to entry into stationary phase (Figure 1D). This drop-off in *P1rrnB* activity correlated with the large increase in cipro persistence observed in high-density cultures (Figure 1C). *P1rrnB* activity can be modulated by starvation signaling through the stringent response or, alternatively, by the depletion of cellular energy stores from nucleic acid triphosphate molecules (ATP, GTP) (Paul et al., 2004).

As this ribosomal promoter element has been used as a proxy for persister cells (Maisonneuve et al., 2013), we applied this system to explore the contribution of the guanosine tetraphosphate (ppGpp)-mediated stringent response on DDP to cipro. Persistence of *E. coli* to bactericidal antibiotics, including cipro, has been linked with the stringent response, which is modulated by production of high levels of ppGpp by the enzymes RelA and SpoT. We investigated the contribution of the *E. coli* stringent response to DDP to cipro using ppGpp⁰ strain $\Delta relAspoT$. Consistent with previous data (Maisonneuve et al., 2013), we found that a stationary-phase $\Delta relAspoT$ mutant displayed a 5.5-fold reduction in persister cells compared to wild-type (Figure 1E). We next assessed the accumulation of persister cells over varying cell densities in the $\Delta relAspoT$ background. Though the total number of persister cells is reduced relative to wild-type, the $\Delta relAspoT$ mutant retains a marked DDP phenotype (Figure 1F). We measured the activity of the *P1rrnB* promoter in the $\Delta relAspoT$ background, and the effective drop in expression occurring in stationary phase was independent of the production of ppGpp (Figure S1I). These findings suggest that starvation itself, rather than the induction of the stringent response, is critical for DDP to cipro.

Both Carbon and Oxygen Are Necessary to Sensitize Stationary-Phase Cells to Cipro

We next sought to elucidate the factors limiting cell death at high cell density. To have greater control on the metabolic inputs in the culture, we used defined MOPS-rich media for these experiments. We first assessed if stationary-phase carbon depletion

was responsible for DDP to cipro. Consistent with earlier reports (Allison et al., 2011), addition of glucose to stationary-phase cultures promoted minimal increases of cipro activity. Sensitization to 1 $\mu\text{g/mL}$ of cipro by glucose was dose dependent starting at 0.4% with a plateau at 1% glucose (Figure 2A).

Because oxygen is a known limiting growth factor at high cell density (Losen et al., 2004) and a known variable limiting quinolone sensitivity (Lewin et al., 1991), we next evaluated the effect of media oxygenation on cipro activity in the presence and absence of supplementary glucose. To this end, we measured and modulated steady-state oxygen concentrations in static culture systems (Figures 2A and 2B). Using this approach, we first examined stationary-phase cell sensitivity to cipro in static culture (Figure 2A). Notably, static cultures displayed the identical DDP to cipro (Figure 2C). Importantly, we observed that static cultures receiving no aeration showed no sensitization to glucose supplementation (Figures 2A and 2D). This observation suggested the possibility that glucose supplementation can partially restore the activity of quinolone antibiotics only under aerated growth conditions.

To further explore aeration-dependent cipro activity, we measured dissolved oxygen as a function of growth density using a solid-state oxygen detector sensitive to molecular oxygen at 8 ppb under static growth conditions (Figure 2B). We found that dissolved oxygen dropped below the detection limit at 220 min of growth, corresponding to a population density of 5×10^7 cells, or 5% of maximal growth. Continuous monitoring of stationary-phase cultures in static growth conditions showed that dissolved oxygen levels remained below our detection limit even after 24 hr of static incubation (Figure 2B).

To confirm that bacterial cells were responding physiologically to changes in oxygen tension as culture density increased, consistent with an aerobic-to-anaerobic transition, we measured gene expression of two genes known to be differentially regulated by the oxygen concentration. Using qPCR, we compared the expression of the main cytochrome oxidase (*cyoA*) and the anaerobic fumarate reductase gene (*frdA*) to the expression of the housekeeping gene *zwf* (Tseng et al., 1996) (Figure 2D). We found expression patterns typical of an aerobic-to-anaerobic shift, demonstrating progressive *cyoA* downregulation and increasing *frdA* expression as the population density increased. Thus, in static culture (Figure 2D), as cell density increases, the bacterial population adapts physiologically by reorganizing its electron transport chain in a manner consistent with reduced oxygen availability, further suggesting that oxygen starvation is present in high-density cultures.

To test the hypothesis that both carbon and oxygen constitute simultaneous limiting factors in DDP to cipro, we evaluated antibiotic susceptibility of static cultures receiving defined oxygen supplementation. We provided oxygen by bubbling filtered air into the media at a calibrated rate (10 psi) to maintain a steady-state oxygen tension of 5%–6% in the static stationary-phase cultures. Consistent with our hypothesis, we found that stationary-phase *E. coli* was highly susceptible to cipro when exposed to a combination of glucose and oxygen, while addition of glucose or oxygen alone had minimal effect (Figure 2E). Under this specific level of glucose supplementation (0.4%), the degree of killing under static conditions with oxygen supplementation

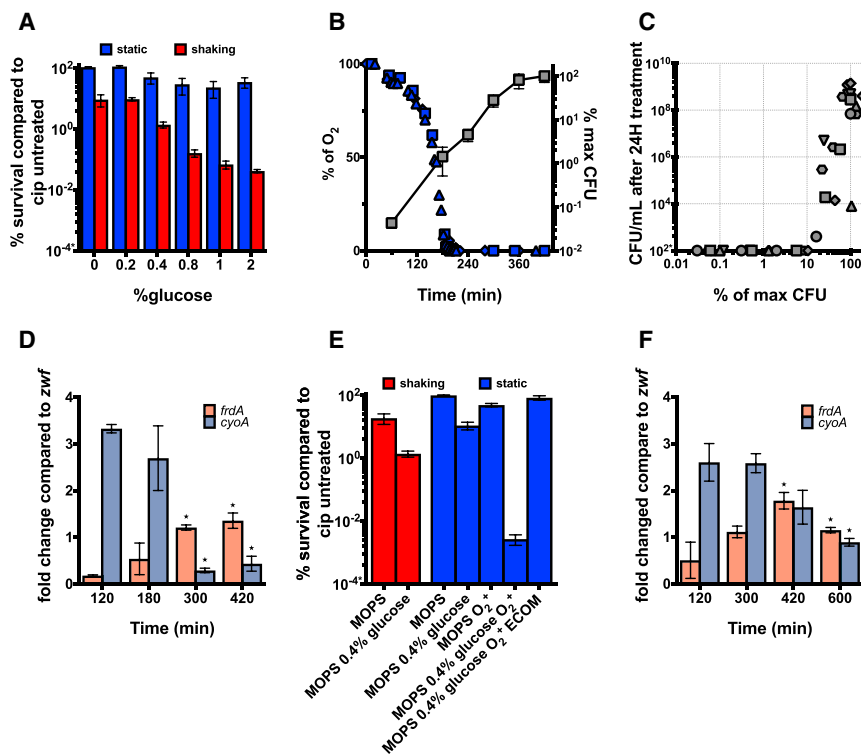


Figure 2. *E. coli* Dissolved Oxygen Concentration Limits Cipro Sensitivity at High Cell Density

(A) Glucose-dependent sensitization to 1 $\mu\text{g}/\text{mL}$ of cipro in stationary-phase shaking (red bar) or static (blue bar) culture (mean \pm SEM, $n = 3$).

(B) Dissolved oxygen concentration (left axis) compared with growth in *E. coli* static culture (right axis; mean \pm SEM, $n = 5$).

(C) Density-dependent persistence to cipro in *E. coli* static culture. Gray squares indicate % max CFU; blue shapes indicate % of O₂.

(D) Expression of the *frdA* and *cyoA* mRNA compared to the reference *zwf* in static culture (mean \pm SEM, $n = 3$).

(E) Aeration-dependent sensitization of *E. coli* static culture by glucose to 1 $\mu\text{g}/\text{mL}$ of cipro (mean \pm SEM, $n = 4$).

(F) Expression of the *frdA* and *cyoA* mRNA compared to the reference *zwf* in shaking culture (mean \pm SEM, $n = 3$).

In (A), (C), and (E), 10^{-4} and 10^2 show our limit of detection. In (B) and (C), each symbol represents a different biological replicate. In (D) and (F), * indicates unpaired *t* test comparison to the 120 min time point; $p < 0.05$.

exceeded killing found in the optimized shaking condition (Figures 2A and 2E). We next assessed the influence of this treatment on cipro uptake and found no difference between control and metabolite-supplemented cultures (Figure S2A). Taken together, these data suggest that DDP to cipro in static growth conditions is mediated by blocks to cellular respiration imposed by limitations in both carbon and oxygen and that supply of these two factors is sufficient to sensitize high-density cultures to cipro. To further assess this hypothesis, we attempted to sensitize a well-characterized *E. coli* strain (ECOM) that is limited to fermentative metabolism under aerobic conditions due to deletion of the complete cytochrome oxidase loci and a quinol monooxygenase (Portnoy et al., 2008). This strain is genetically incapable of coupling molecular oxygen to oxidative phosphorylation. Consistent with our hypothesis, the ECOM strain was insensitive to cipro at high density when provided supplemental glucose and oxygen (Figures 2E, S2B, and S2C).

Since we observed increased killing in the oxygen-supplemented static cultures relative to shaking cultures (Figures 2A and 2E), we hypothesized that aeration may be limited even under optimized shaking conditions and thus that oxygen may be a limiting factor in this setting. Due to the physical constraints of the system, we were not able to confidently measure dissolved oxygen in our shaking conditions with the oxygen probe. As a proxy for aero-anaerobic transition, we evaluated the expression levels of *cyoA* and *frdA* in shaking cultures and found that *cyoA* and *frdA* expression patterns were similar in both shaking and static cultures, further suggesting that oxygen tension is limiting even when cultures are optimally aerated by shaking (Figure 2F).

Fumarate Can Substitute Oxygen as an Electron Acceptor to Sensitize Bacteria to Cipro

The *E. coli* respiration system is highly versatile, and the quinol pool can transfer electrons to substrates other than oxygen. We asked if anaerobic respiration could also lead to glucose-dependent sensitization to cipro in stationary phase. We tested nitrate, DMSO, and fumarate as alternative electron acceptors in MOPS-rich media under shaking conditions (Figure 3A). While none of these electron acceptors alone was able to sensitize cells to cipro, we found that in combination with glucose, fumarate synergistically sensitized high-density cultures to 1 $\mu\text{g}/\text{mL}$ cipro in a manner similar to oxygen supplementation (Figures 3A, S3A, and S3B). Similar synergy was observed using the third- and fourth-generation quinolone antibiotics, levofloxacin and moxifloxacin, respectively (Figure S3F), indicating conservation of the phenotype across the chemical generations of quinolones. Increasing glucose above 0.2% did not enhance killing in conjunction with fumarate (Figure S3A), indicating again that carbon source availability is required, but not strictly limiting, for DDP to cipro.

We next assessed the dose-dependent relationship of cipro sensitization to the combination of glucose and fumarate. While sensitization was limited to concentrations above 500 ng/mL of cipro for the MOPS-rich media (Figure 3B), stationary-phase cells grown in LB supplemented with glucose and fumarate were killed by cipro at concentrations as low as 50 ng/mL (Figure 3C).

As our data suggested that cellular respiration was a limiting factor for sensitization by glucose, we wanted to confirm that in our condition cells used fumarate as a terminal electron acceptor. We thus tested cipro sensitivity at high cell density

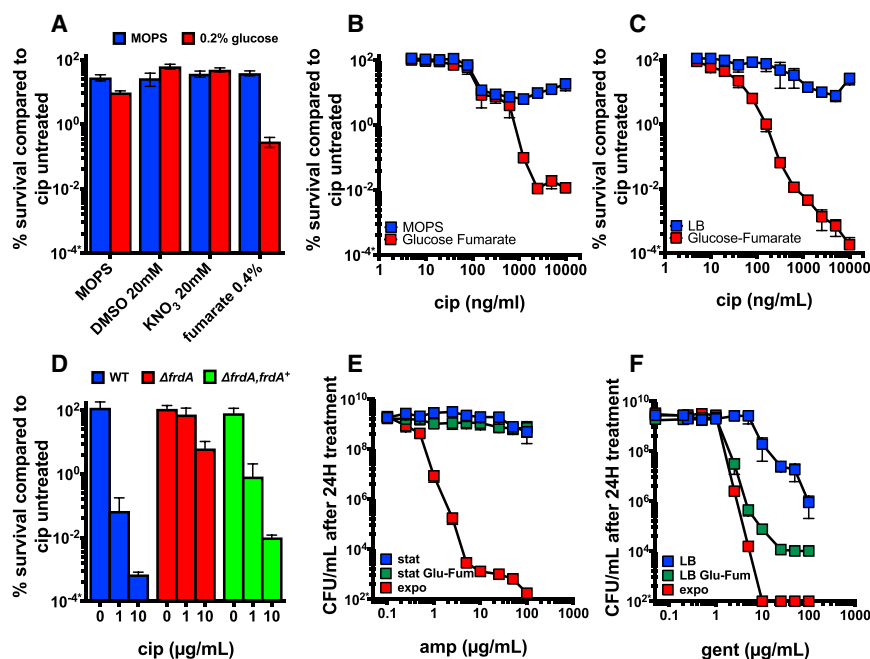


Figure 3. Fumarate Respiration-Dependent Sensitization to Cipro by Glucose

(A) Alternative electron acceptors synergize glucose sensitization to 1 $\mu\text{g}/\text{mL}$ of cipro in shaking MOPS stationary-phase culture.

(B) Glucose-fumarate (0.2%–0.2%) synergy across cipro concentrations in shaking MOPS stationary-phase culture.

(C) Glucose-fumarate (0.2%–0.2%) synergy across cipro concentrations in shaking LB stationary-phase culture.

(D) The glucose-fumarate synergy depends on the fumarate reductase activity.

(E and F) Glucose-fumarate sensitization to different concentrations of gentamicin (E) and ampicillin (F) (mean \pm SEM, $n = 3$); 10^{2*} shows our limit of detection.

In (A)–(D), data represent the mean \pm SEM, $n = 3$, of the percent survival compared to cipro untreated; 10^{-4*} shows our limit of detection.

of a mutant strain lacking the catalytic subunit of the fumarate reductase gene, *frdA*. We found that the *frdA* mutant was not able to be sensitized to cipro killing by the combination glucose-fumarate, suggesting a direct role of alternative respiration through fumarate reduction as a key factor in sensitizing cells to cipro (Figures 3D and S3B). Complementation of the *frdA* mutant using a plasmid expressing the *frdA* gene under the control of the native promoter restored sensitization to cipro by glucose and fumarate supplementation (Figure 3D).

We next sought to better understand how the enzymatic reduction of fumarate leads to cell death by cipro. We hypothesized that the addition of fumarate was sensitizing cells by specifically increasing cellular respiration (Figure 2E) as a component of overall cellular metabolism rather than simply driving cell division. Although we did not observe a significant increase in CFU over time after the addition of glucose and fumarate (Figure S3C), we decided to use a more sensitive method to differentiate cellular respiration and cell growth. To assess this, we asked whether glucose-fumarate supplementation could sensitize stationary-phase cells to ampicillin (Figure 3E), a β -lactam antibiotic that requires cell division for killing, or gentamicin (Figure 3F), which requires an active metabolism and the generation of a proton motive force for drug uptake. Confirming our original hypothesis, glucose-fumarate supplementation sensitized stationary-phase *E. coli* to gentamicin; however, even high concentrations of ampicillin did not kill stationary-phase cells with glucose-fumarate supplementation, further supporting the hypothesis that metabolite addition was not inducing significant cell growth in high-density cultures.

Carbon Source and Electron Acceptor Availability Limits Cipro Activity in *S. aureus* and *M. smegmatis*

Having defined a mechanistic context for DDP to cipro in a Gram-negative enterobacterium, we next tested whether our findings

were generalizable to two additional bacteria, *S. aureus* (MIC: 250 $\mu\text{g}/\text{mL}$) and *M. smegmatis* (MIC: 500 ng/ml). Though cipro alone was not as potent for treating *S. aureus* and *M. smegmatis* in exponentially growing cultures as for *E. coli*, higher doses could successfully reduce the number of viable cells below the limit of detection for both species (Figures 4A and 4B). Similar to *E. coli*, *S. aureus* and *M. smegmatis* exhibit marked DDP to cipro upon entry into stationary phase (Figures 4A and 4B).

Because the *M. smegmatis* genome includes several putative fumarate reductase enzymes (Caspi et al., 2016), we attempted to sensitize aerated stationary-phase cultures to cipro by using a combination of glucose and fumarate (Figure 4C). We found that while 0.4% fumarate or 0.4% glucose alone could sensitize cultures weakly, the combination of both compounds strongly sensitized *M. smegmatis* stationary-phase cultures. *S. aureus* is not able to use fumarate as an alternative electron acceptor (Fuchs et al., 2007). Thus, we tried sensitizing *S. aureus* stationary cultures to cipro by the combination of oxygen and glucose (Figure 4D). While the addition of glucose or bubbling had a limited effect on cipro activity, the addition of 0.4% glucose together with bubbling sensitized *S. aureus* static cultures to 5 and 10 $\mu\text{g}/\text{mL}$ of cipro. These observations indicate that the stimulation of metabolism specifically at the level of cellular respiration is a broadly applicable method to sensitize a range of bacteria to cipro.

DISCUSSION

DDP to quinolone antibiotics is a known phenotype without a defined mechanism (Zeiler, 1985). Here we show that external limits to specific metabolic pathways, rather than the cellular response to starvation, are the key factors modulating quinolone activity under high-cell-density conditions. While carbon sources are limiting, replenishment of carbon oxidation pathways alone is insufficient for cipro activity, and the availability

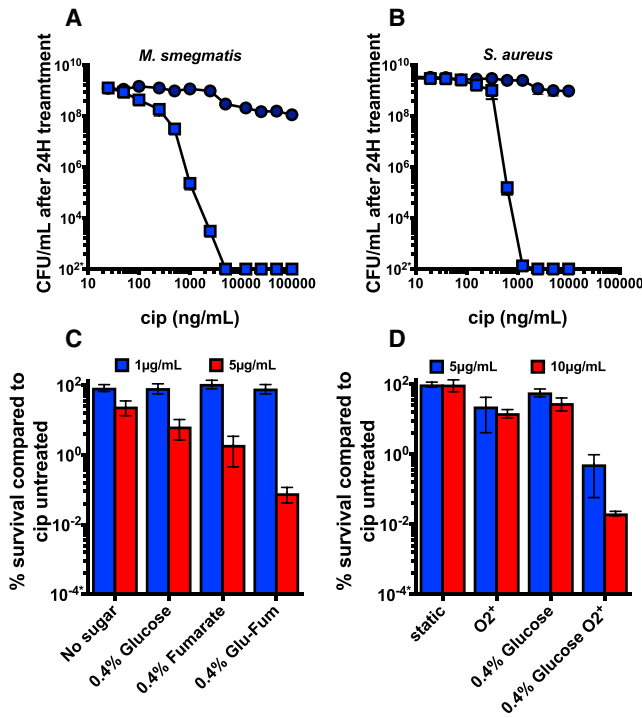


Figure 4. Sensitization to Cipro in Clinically Relevant Pathogens (A and B) Density-dependent persistence to cipro in *M. smegmatis* (A) and *S. aureus* (B); dark blue circle corresponds to stationary-phase cells and blue square corresponds to cells treated at 1% maximal density; 10²⁺ shows our limit of detection. (C) Glucose-fumarate sensitization of shaking stationary-phase *M. smegmatis* culture to cipro. (D) Aeration-dependent glucose sensitization of static stationary-phase *S. aureus*. 10⁻⁴⁺ shows our limit of detection. (A) and (B) show mean ± SEM, n = 3; (C) and (D) show mean ± SEM, n = 3 of percent survival compared to cipro untreated.

of a suitable terminal electron acceptor is critical to regenerate lethal activity of quinolone antibiotics in high cell-density settings. With this framework, we propose a simple, two-input metabolite-driven strategy to stimulate the activity of cipro against a range of bacteria at high densities. The implications for therapeutic implementation of this strategy warrant further studies.

An emerging model for bacterial persistence to antibiotics has focused on physiologic adaptation to starvation, as mediated by the stringent response (Harms et al., 2016). A key finding from our work, in particular using a ppGpp⁰ strain, is that starvation itself rather than cellular adaptations to starvation is the major driving force in DDP. Antibiotic persistence has been described to derive from two physiologic processes that are either induced or stochastic, referred to as type I and type II persisters (Levin-Reisman and Balaban, 2016). In our work, it is important to note that we have focused on induced, type I persisters specifically and that conclusions drawn here cannot necessarily be applied to stochastically formed persisters, which exist in our sensitized cultures after treatment.

While *E. coli* can oxidize carbon and generate ATP through fermentation, we find that cell killing by cipro requires activity

of respiratory metabolic pathways, which can be accomplished by a limited number of metabolic inputs. It is known that topoisomerase activity is ATP dependent and that stationary-phase cells require topoisomerases to recover supercoiling (Gutiérrez-Estrada et al., 2014), suggesting that starvation states may limit the activity of these enzymes. Furthermore, increased cellular respiration is implicated in antibiotic-mediated cell death through downstream processes (Grant et al., 2012; Lobritz et al., 2015). We hypothesize that priming respiratory metabolism by the addition of a carbon source and electron acceptor affects both target corruption and other, less-characterized, downstream processes to sensitize cells to quinolones. Remarkably, one study has been able to leverage the metabolic stress induced by extreme levels of intracellular fumarate accumulation to promote a broad range of persistence phenotypes (Kim et al., 2016). This work emphasizes the complex interaction between cellular metabolic activity and drug sensitivity.

While previous starvation models have focused on the availability of carbon and nitrogen nutrients in the media (Allison et al., 2011; Amato et al., 2013; Meylan et al., 2017; Nguyen et al., 2011; Shan et al., 2017), we found that high-density static cultures quickly utilize the available dissolved oxygen, rendering this factor limiting in the metabolic process of cellular respiration. By coupling these measurements to expression data of genes that typify the aero-anaerobic transition, *cyoA* and *frdA*, we suspect that oxygen becomes limiting in both aerated and static cultures before entry into stationary phase. In our aerated cultivation system with *E. coli*, we detect an increase in persistence to cipro when the population reached 1e⁸ cells per milliliter of media (OD₆₀₀ of 0.3) or approximately 10% of the maximal carrying capacity. This is consistent with a well-described change in the growth status of cells in LB media (Sezonov et al., 2007). These findings, combined with the knowledge that the bactericidal activity of drugs such as quinolones is sensitive to the aero-anaerobic transition (Lewin et al., 1991), suggest the importance of both experimental growth conditions and sample handling in assessment of antibiotic sensitivity. Variation of growth conditions applied among laboratories could impact conclusions made in the field of antimicrobial research. We propose that the percent maximal carrying capacity be considered in order to help standardize antibiotic activity assessment.

Although antibiotic persistence has been previously implicated in recurring and chronic infections (Fauvart et al., 2011), it is now also appreciated as an important factor that could affect the spread of resistant bacteria (Levin-Reisman et al., 2017). Antibiotics from the quinolone family are a significant component of the arsenal against bacterial infectious diseases. However, a SNP within one of the gyrase subunits can increase the MIC of quinolones by orders of magnitude (Levy et al., 2004). It is important to note that persistence displayed by high-cell-density populations could also be subject to selection through adaptive mutagenesis (Lauret et al., 2013). Thus, it is critical that we more thoroughly understand the mechanistic underpinnings of antibiotic persistence, so that rational approaches to the deployment of our antibiotic arsenal can be achieved (Smith and Romesberg, 2007).

STAR★METHODS

Detailed methods are provided in the online version of this paper and include the following:

- KEY RESOURCES TABLE
- CONTACT FOR REAGENT AND RESOURCE SHARING
- EXPERIMENTAL MODEL AND SUBJECT DETAILS
- METHOD DETAILS
 - Chemical preparation
 - Knockout construction
 - Plasmid construction
 - Density-persistence assay
 - Potentiation assays
 - Dilution assay
 - Fluorescent reporter measurements
 - Oxygen probe measurements
 - qPCR
 - Ciprofloxacin uptake measurements
- QUANTIFICATION AND STATISTICAL ANALYSIS

SUPPLEMENTAL INFORMATION

Supplemental Information includes three figures and can be found with this article online at <https://doi.org/10.1016/j.molcel.2017.11.012>

ACKNOWLEDGMENTS

This work was supported by the Defense Threat Reduction Agency grant HDTRA1-15-1-0051, the Broad Institute of MIT and Harvard, and a generous gift from Anita and Josh Bekenstein. We would like to thank the Palsson lab from UC San Diego for sharing the ECOM4LA strain.

AUTHOR CONTRIBUTIONS

Conceptualization, A.G.; Methodology, A.G., S.J.; Investigation, A.G., S.J., P.B., M.H.; Writing – Original draft, A.G., S.J.; Writing – editing, P.B., M.A.L., J.J.C.; Supervision and funding acquisition, J.J.C.

DECLARATION OF INTERESTS

J.J.C. is scientific co-founder and SAB chair of EnBiotix, which is an antibiotic drug discovery company.

Received: June 23, 2017

Revised: October 11, 2017

Accepted: November 10, 2017

Published: December 7, 2017

REFERENCES

- Allison, K.R., Brynildsen, M.P., and Collins, J.J. (2011). Metabolite-enabled eradication of bacterial persisters by aminoglycosides. *Nature* **473**, 216–220.
- Amato, S.M., Orman, M.A., and Brynildsen, M.P. (2013). Metabolic control of persister formation in *Escherichia coli*. *Mol. Cell* **50**, 475–487.
- Asuquo, A.E., and Piddock, L.J. (1993). Accumulation and killing kinetics of fifteen quinolones for *Escherichia coli*, *Staphylococcus aureus* and *Pseudomonas aeruginosa*. *J. Antimicrob. Chemother.* **31**, 865–880.
- Balaban, N.Q., Gerdes, K., Lewis, K., and McKinney, J.D. (2013). A problem of persistence: still more questions than answers? *Nat. Rev. Microbiol.* **11**, 587–591.
- Barraud, N., Buson, A., Jarolimek, W., and Rice, S.A. (2013). Mannitol enhances antibiotic sensitivity of persister bacteria in *Pseudomonas aeruginosa* biofilms. *PLoS ONE* **8**, e84220.
- Brauner, A., Fridman, O., Gefen, O., and Balaban, N.Q. (2016). Distinguishing between resistance, tolerance and persistence to antibiotic treatment. *Nat. Rev. Microbiol.* **14**, 320–330.
- Bush, K., Courvalin, P., Dantas, G., Davies, J., Eisenstein, B., Huovinen, P., Jacoby, G.A., Kishony, R., Kreiswirth, B.N., Kutter, E., et al. (2011). Tackling antibiotic resistance. *Nat. Rev. Microbiol.* **9**, 894–896.
- Caspi, R., Billington, R., Ferrer, L., Foerster, H., Fulcher, C.A., Keseler, I.M., Kothari, A., Krummenacker, M., Latendresse, M., Mueller, L.A., et al. (2016). The MetaCyc database of metabolic pathways and enzymes and the BioCyc collection of pathway/genome databases. *Nucleic Acids Res.* **44** (D1), D471–D480.
- Conlon, B.P., Rowe, S.E., Gandt, A.B., Nuxoll, A.S., Donegan, N.P., Zalis, E.A., Clair, G., Adkins, J.N., Cheung, A.L., and Lewis, K. (2016). Persister formation in *Staphylococcus aureus* is associated with ATP depletion. *Nat. Microbiol.* **1**, 16051.
- Dörr, T., Lewis, K., and Vulić, M. (2009). SOS response induces persistence to fluoroquinolones in *Escherichia coli*. *PLoS Genet.* **5**, e1000760.
- Dörr, T., Vulić, M., and Lewis, K. (2010). Ciprofloxacin causes persister formation by inducing the TisB toxin in *Escherichia coli*. *PLoS Biol.* **8**, e1000317.
- Drlica, K., Malik, M., Kerns, R.J., and Zhao, X. (2008). Quinolone-mediated bacterial death. *Antimicrob. Agents Chemother.* **52**, 385–392.
- Dwyer, D.J., Belenky, P.A., Yang, J.H., MacDonald, I.C., Martell, J.D., Takahashi, N., Chan, C.T., Lobritz, M.A., Braff, D., Schwarz, E.G., et al. (2014). Antibiotics induce redox-related physiological alterations as part of their lethality. *Proc. Natl. Acad. Sci. USA* **111**, E2100–E2109.
- Dwyer, D.J., Collins, J.J., and Walker, G.C. (2015). Unraveling the physiological complexities of antibiotic lethality. *Annu. Rev. Pharmacol. Toxicol.* **55**, 313–332.
- Fauvar, M., De Groote, V.N., and Michiels, J. (2011). Role of persister cells in chronic infections: clinical relevance and perspectives on anti-persister therapies. *J. Med. Microbiol.* **60**, 699–709.
- Fuchs, S., Pané-Farré, J., Kohler, C., Hecker, M., and Engelmann, S. (2007). Anaerobic gene expression in *Staphylococcus aureus*. *J. Bacteriol.* **189**, 4275–4289.
- Grant, S.S., Kaufmann, B.B., Chand, N.S., Haseley, N., and Hung, D.T. (2012). Eradication of bacterial persisters with antibiotic-generated hydroxyl radicals. *Proc. Natl. Acad. Sci. USA* **109**, 12147–12152.
- Gutiérrez-Estrada, A., Ramírez-Santos, J., and Gómez-Eichelmann, Mdel.C. (2014). Role of chaperones and ATP synthase in DNA gyrase reactivation in *Escherichia coli* stationary-phase cells after nutrient addition. *Springerplus* **3**, 656.
- Harms, A., Maisonneuve, E., and Gerdes, K. (2016). Mechanisms of bacterial persistence during stress and antibiotic exposure. *Science* **354**, aaf4268.
- Kim, J.S., Cho, D.H., Heo, P., Jung, S.C., Park, M., Oh, E.J., Sung, J., Kim, P.J., Lee, S.C., Lee, D.H., et al. (2016). Fumarate-Mediated Persistence of *Escherichia coli* against Antibiotics. *Antimicrob. Agents Chemother.* **60**, 2232–2240.
- Knudsen, G.M., Ng, Y., and Gram, L. (2013). Survival of bactericidal antibiotic treatment by a persister subpopulation of *Listeria monocytogenes*. *Appl. Environ. Microbiol.* **79**, 7390–7397.
- Lauret, L., Matic, I., and Gutierrez, A. (2013). Bacterial Responses and Genome Instability Induced by Subinhibitory Concentrations of Antibiotics. *Antibiotics (Basel)* **2**, 100–114.
- Levin-Reisman, I., and Balaban, N.Q. (2016). Quantitative Measurements of Type I and Type II Persisters Using ScanLag. *Methods Mol. Biol.* **1333**, 75–81.
- Levin-Reisman, I., Ronin, I., Gefen, O., Braniss, I., Shosh, N., and Balaban, N.Q. (2017). Antibiotic tolerance facilitates the evolution of resistance. *Science* **355**, 826–830.
- Levy, D.D., Sharma, B., and Cebula, T.A. (2004). Single-nucleotide polymorphism mutation spectra and resistance to quinolones in *Salmonella enterica* serovar Enteritidis with a mutator phenotype. *Antimicrob. Agents Chemother.* **48**, 2355–2363.

- Lewin, C.S., Morrissey, I., and Smith, J.T. (1991). The mode of action of quinolones: the paradox in activity of low and high concentrations and activity in the anaerobic environment. *Eur. J. Clin. Microbiol. Infect. Dis.* *10*, 240–248.
- Lobritz, M.A., Belenky, P., Porter, C.B., Gutierrez, A., Yang, J.H., Schwarz, E.G., Dwyer, D.J., Khalil, A.S., and Collins, J.J. (2015). Antibiotic efficacy is linked to bacterial cellular respiration. *Proc. Natl. Acad. Sci. USA* *112*, 8173–8180.
- Losen, M., Frölich, B., Pohl, M., and Büchs, J. (2004). Effect of oxygen limitation and medium composition on *Escherichia coli* fermentation in shake-flask cultures. *Biotechnol. Prog.* *20*, 1062–1068.
- Maisonneuve, E., Castro-Camargo, M., and Gerdes, K. (2013). (p)ppGpp controls bacterial persistence by stochastic induction of toxin-antitoxin activity. *Cell* *154*, 1140–1150.
- Mathieu, A., Fleurier, S., Frénoy, A., Dairou, J., Bredeche, M.F., Sanchez-Vizueté, P., Song, X., and Matic, I. (2016). Discovery and Function of a General Core Hormetic Stress Response in *E. coli* Induced by Sublethal Concentrations of Antibiotics. *Cell Rep.* *17*, 46–57.
- Meylan, S., Porter, C.B., Yang, J.H., Belenky, P., Gutierrez, A., Lobritz, M.A., Park, J., Kim, S.H., Moskowitz, S.M., and Collins, J.J. (2017). Carbon Sources Tune Antibiotic Susceptibility in *Pseudomonas aeruginosa* via Tricarboxylic Acid Cycle Control. *Cell Chem. Biol.* *24*, 195–206.
- Moyed, H.S., and Bertrand, K.P. (1983). *hipA*, a newly recognized gene of *Escherichia coli* K-12 that affects frequency of persistence after inhibition of murein synthesis. *J. Bacteriol.* *155*, 768–775.
- Nguyen, D., Joshi-Datar, A., Lepine, F., Bauerle, E., Olakanmi, O., Beer, K., McKay, G., Siehnel, R., Schafhauser, J., Wang, Y., et al. (2011). Active starvation responses mediate antibiotic tolerance in biofilms and nutrient-limited bacteria. *Science* *334*, 982–986.
- Paul, B.J., Ross, W., Gaal, T., and Gourse, R.L. (2004). rRNA transcription in *Escherichia coli*. *Annu. Rev. Genet.* *38*, 749–770.
- Peng, B., Su, Y.B., Li, H., Han, Y., Guo, C., Tian, Y.M., and Peng, X.X. (2015). Exogenous alanine and/or glucose plus kanamycin kills antibiotic-resistant bacteria. *Cell Metab.* *21*, 249–261.
- Portnoy, V.A., Herrgård, M.J., and Palsson, B.O. (2008). Aerobic fermentation of D-glucose by an evolved cytochrome oxidase-deficient *Escherichia coli* strain. *Appl. Environ. Microbiol.* *74*, 7561–7569.
- Prax, M., Mechler, L., Weidenmaier, C., and Bertram, R. (2016). Glucose Augments Killing Efficiency of Daptomycin Challenged *Staphylococcus aureus* Persisters. *PLoS ONE* *11*, e0150907.
- Sezonov, G., Joseleau-Petit, D., and D'Ari, R. (2007). *Escherichia coli* physiology in Luria-Bertani broth. *J. Bacteriol.* *189*, 8746–8749.
- Shan, Y., Brown Gandt, A., Rowe, S.E., Deisinger, J.P., Conlon, B.P., and Lewis, K. (2017). ATP-Dependent Persister Formation in *Escherichia coli*. *MBio* *8*, e02267.
- Smith, P.A., and Romesberg, F.E. (2007). Combating bacteria and drug resistance by inhibiting mechanisms of persistence and adaptation. *Nat. Chem. Biol.* *3*, 549–556.
- Tseng, C.P., Albrecht, J., and Gunsalus, R.P. (1996). Effect of microaerophilic cell growth conditions on expression of the aerobic (*cyoABCDE* and *cydAB*) and anaerobic (*narGHJL*, *frdABCD*, and *dmsABC*) respiratory pathway genes in *Escherichia coli*. *J. Bacteriol.* *178*, 1094–1098.
- Van den Bergh, B., Fauvart, M., and Michiels, J. (2017). Formation, physiology, ecology, evolution and clinical importance of bacterial persisters. *FEMS Microbiol. Rev.* *41*, 219–251.
- Zeiler, H.J. (1985). Evaluation of the in vitro bactericidal action of ciprofloxacin on cells of *Escherichia coli* in the logarithmic and stationary phases of growth. *Antimicrob. Agents Chemother.* *28*, 524–527.

STAR★METHODS

KEY RESOURCES TABLE

REAGENT or RESOURCE	SOURCE	IDENTIFIER
Bacterial and Virus Strains		
<i>Escherichia coli</i> MG1655	<i>E. coli</i> Genetic Stock Center	CGSC# 6300
<i>Escherichia coli</i> ECOM: Δ cydAB Δ cyoABCD Δ cbdAB Δ ygiN	Portnoy et al., 2008	ECOM4LA
<i>Staphylococcus aureus</i>	ATCC	25923
<i>Mycobacterium smegmatis</i> MC2 155	Hung lab	MC ² 155
MG1655 Δ frdA	This paper	N/A
MG1655 Δ frdA PfrdA::frdA-cat	This paper	N/A
MG1655 Δ relA Δ spoT	Mathieu et al., 2016	N/A
Chemicals, Peptides, and Recombinant Proteins		
LB Broth	Difco	Lot #5202513
MOPS media	Technova	N/A
7H10 media	Difco	Lot #5097702
Ciprofloxacin	Sigma	#17850
Levofloxacin	Sigma	#28266
Gentamicin	Sigma	#G1264
Ampicillin	Sigma	#A9518
Moxifloxacin	Sigma	#SML1581
Glucose	Fisher Scientific	#D16
Fumarate	Sigma	#F1506
Potassium nitrate	Sigma	#P8394
DMSO	ThermoFisher	#85190
Oligonucleotides		
cyoA forward primer for QPCR: GGTACTTCCAGGCGAAACCA	This paper	N/A
cyoA reverse primer for QPCR: TTGGTCTGGAGCAACGTTC	This paper	N/A
frdA forward primer for QPCR: TACGTTGACGCTACCATCCG	This paper	N/A
frdA reverse primer for QPCR: TATTTTCGTCCACCACTGCC	This paper	N/A
zwf forward primer for QPCR: TGCCGCTTTATCCCAGTCAG	This paper	N/A
zwf reverse primer for QPCR: GCGTCGTAAATTGCTGCCTT	This paper	N/A
Primer to clone frdA promoter into pZE backbone, forward: GATA CTCGAG ATCAAACAGCGGTGGG	This paper	N/A
Primer to clone frdA promoter into pZE backbone, reverse: GTAT GAATTC GACATTCCTCCAGATTGT	This paper	N/A
Primer to clone frdA gene into pZE backbone, forward: ctga GGTACCgtgCAAACCTTTCAAGC	This paper	N/A
Primer to clone frdA gene into pZE backbone, reverse: gtca ggatcc tcaGCCATTGCCT	This paper	N/A
frdA forward sequencing: GTGCAAACCTTTCAAGC	This paper	N/A
frdA reverse sequencing: TCAGCCATTGCCTTC	This paper	N/A
frdA promoter forward sequencing: ATCAAACAGCGGTGGG	This paper	N/A
Recombinant DNA		
Plasmid: P1rrnB-GFP-kan	Mathieu et al., 2016	N/A
Plasmid: PfrdA::frdA-cat	This paper	N/A

CONTACT FOR REAGENT AND RESOURCE SHARING

Further information and requests for resources and reagents should be directed to and will be fulfilled by the lead contact, James Collins (jimjc@mit.edu).

EXPERIMENTAL MODEL AND SUBJECT DETAILS

The strains used for this study were *E. coli* K12 strain MG1655, *S. aureus* strain ATCC 25923 and *M. smegmatis* strain mc² 155. *E. coli* MG1655 was provided by the *E. coli* Genetic Stock Center database. *S. aureus* was provided by ATCC. *M. smegmatis* was provided by Deborah Hung's lab. *E. coli* and *S. aureus* were grown in Luria Broth (LB, Difco) medium and MOPS EZ Rich (MOPS, Teknova) medium supplemented with 0.2% glucose. *M. smegmatis* was grown in Middlebrook 7H9 supplemented with 0.05% oleic acid, 2% dextrose, and 0.004% catalase (OADC). All cells were grown at 37°C.

METHOD DETAILS

Chemical preparation

Antibiotics stock solutions were made as follows: ciprofloxacin was dissolved to 10mg/mL in 0.1M NaOH; levofloxacin was dissolved in glacial acetic acid; gentamicin, ampicillin, and moxifloxacin were dissolved to 10mg/mL in water. All metabolites were dissolved in water to the following stock solutions: 40%w/v glucose, 20%w/v fumarate, 1M potassium nitrate.

Knockout construction

E. coli genetic knockouts $\Delta recB$ and $\Delta frdA$ were constructed by P1 transduction from the Keio collection. Knockout strains were checked for accuracy by PCR amplification and gel electrophoresis.

Plasmid construction

The pZE21 backbone was used for construction of all plasmids (see [Key Resources Table](#)). The kan cassette in the pZE21 was replaced with the Cm^R cassette flanked by FRT sites from the pKD3 vector. The *frdA* promoter replaced the tet promoter through the *xhoI* and *kpnI* cut sites. The *mcherry* gene was replaced by *frdA* using the *kpnI* and *hindIII* cut sites. These plasmids were selected by 35 μ g/mL chloramphenicol. The P1::*rrnB-gfp* plasmid was made directly from the pZE21-*mcherry* backbone and selected on 50 μ g/mL kanamycin. Plasmids were transformed into background strains using CaCl₂ transformation.

Density-persistence assay

An overnight culture of *E. coli* was diluted 1/10,000 in MOPS or LB in either (a) a non-baffled flask in the shaking incubator, 37°C, 300 rpm (shaking condition), or (b) in 30mL in a 100mL bottle in a 37°C water bath (static condition). At varying time points throughout growth, 1mL of cells were moved to a culture tube and treated with 1 μ g/mL ciprofloxacin added by pipetting; the tubes were placed in shaking or static conditions, respectively. At each time point, cells were also serially diluted in PBS and plated on LB agar plates to determine the CFU/mL at the time of treatment. Time points were taken until cells reached maximum carrying capacity. After 24 hr of treatment, 100 μ L of cells from each tube was spun down and re-suspended in PBS on a 96-well plate. Cells were then serially diluted and plated on LB agar plates. The CFU/mL at treatment was normalized by the CFU/mL of stationary phase cells (%max CFU/mL).

Potentiation assays

Cells were grown for 24 hr in either (a) a non-baffled flask overnight in the shaking incubator, 37°C, 300 rpm (shaking condition), or (b) in 30mL in a 100mL bottle in a 37°C water bath (static condition). For the shaking condition, the volume of culture was set to a tenth of the flask volume. For potentiation via metabolites, 1mL of culture was allocated to 14mL culture tubes and treated with varying concentrations of ciprofloxacin, sugars, and electron acceptors. After 24 hr of treatment, 100 μ L of cells were spun down for 5min at 3500rpm in a 96-well plate. Cells were re-suspended in PBS and serially diluted in PBS by 10-fold. *E. coli* and *S. aureus* were spotted on LB Agar (Difco) plates; *M. smegmatis* was spotted on 7H10(Difco)+10%v/v OADC supplement (Hardy Diagnostics) plates. The plates were incubated at 37°C and colonies were counted, reported as colony-forming units per mL (CFU/ml). For potentiation with oxygen, filtered air was bubbled (10 psi) into cells grown in the static condition for 24 hr with or without glucose. These cells were then spun down and resuspended in PBS, serially diluted and plated on LB agar plates.

Dilution assay

An overnight culture of *E. coli* was diluted 1/10, 1/100, 1/1000, and 1/10000 in non-baffled flasks. The cultures were grown for 1h and treated with either 1 μ g/mL or 10 μ g/mL cipro for 24 hr. Cells were spun down and re-suspended in PBS, diluted and plated on LB agar plates to determine CFU/ml.

Fluorescent reporter measurements

Fluorescence was measured by a SpectraMax M3 Microplate Reader spectrophotometer (Molecular Devices). For P1::rnb-gfp signal, an overnight culture of cells was diluted 1/10,000 in MOPS or LB containing 50 $\mu\text{g}/\text{mL}$ kanamycin. At appropriate time points during growth, 300 μL of cells were moved to a black 96-well plate with clear bottom. The GFP signal was read on the plate reader at an emission/excitation of 488/510 and PMT of 20. At each time point, cells were also serially diluted and plated for CFU/mL determination.

Oxygen probe measurements

Dissolved oxygen in the media was measured using a Mettler Toledo InPro O2 sensor, 68601. The probe was kept in a static culture of cells in a water bath and the probe measured the percent of dissolved oxygen every 5 min.

qPCR

Bacterial pellets were collected and stored using RNeasy Protect (QIAGEN) according to the manufacturer's instructions, and RNA was isolated using the RNeasy RNA isolation kit (QIAGEN). RNA was DNase treated and reverse transcribed with random hexamers using the Verso RT kit (Thermo Fisher Scientific). DNA contamination was tested by PCR of the RNA prep using the qPCR primers. Relative gene expression was determined using SYBR Green 1-based real-time PCR (Roche). Concentrations were calculated from the linear standard curve and all transcripts were normalized to the *zwf* gene expression.

Ciprofloxacin uptake measurements

The protocol was adapted from [Asuquo and Piddock, 1993](#). 1mL of Stationary phase cells was treated with ciprofloxacin and glucose-fumarate at 0.2% for 30min. Cells were then washed 2 times in 2mL ice cold PBS. Ciprofloxacin was extracted using 1mL of glycine-HCl buffer at pH3 for 2H. Cell residues were pelleted by centrifugation and fluorescence was read from the supernatant at 275nm excitation and 410nm emission. The quantity of ciprofloxacin was estimated using ciprofloxacin at defined concentration diluted in glycine-HCl extract from a ciprofloxacin non-treated culture.

QUANTIFICATION AND STATISTICAL ANALYSIS

All graphics and statistical analyses were done using PRISM software version 7. [Figure 1E](#) the comparison between WT and the ppGpp⁰ was tested using two-tailed Mann-Whitney $p = 0.017$ $n = 5$ ppGpp⁰ and $n = 7$ for WT. [Figures 2D](#) and [2E](#), comparison to the 120min time point was using two-tailed unpaired t test; [Figure 2D](#) all significant value: p value < 0.001 . [Figure 2E](#) all significant value: p value < 0.05 .